Journal Pre-proof

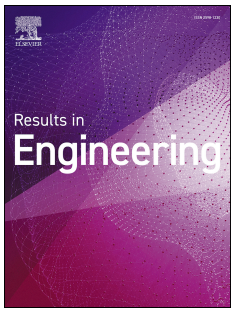

Systematic covalent crosslinking of graphene oxide membranes using 1,3,5 triazine 2,4,6 triamine for enhanced structural intactness and improved nanofiltration performance

Vepika Kandjou, Beatriz Acevedo, Sonia Melendi-Espina

PII: S2590-1230(23)00163-9

DOI: https://doi.org/10.1016/j.rineng.2023.101036

Reference: RINENG 101036

To appear in: *Results in Engineering*

Received Date: 23 January 2023

Revised Date: 14 March 2023

Accepted Date: 16 March 2023

Please cite this article as: V. Kandjou, B. Acevedo, S. Melendi-Espina, Systematic covalent crosslinking of graphene oxide membranes using 1,3,5 triazine 2,4,6 triamine for enhanced structural intactness and improved nanofiltration performance, *Results in Engineering* (2023), doi: https://doi.org/10.1016/j.rineng.2023.101036.

CRediT author statement

Vepika Kandjou: Conceptualization, Drafting, Methodology and Characterisation **Sonia Melendi-Espina**: Conceptualization, Editing and Reviewing. **Beatriz Munoz:** Characterisations and Editing

Systematic covalent crosslinking of graphene oxide membranes using 1,3,5 triazine 2,4,6 triamine for enhanced structural intactness and improved nanofiltration performance

Vepika Kandjou [1, 4*], Beatriz Acevedo [3] and Sonia Melendi-Espina [2]

[1] *Department of Chemical Materials and Metallurgical Engineering (CMME), Botswana International University of Science and Technology (BIUST), P/Bag 16, Palapye, Botswana*

[2] *Engineering, Faculty of Science. University of East Anglia (UEA), Norwich, UK*

[3] *SCK CEN: Belgian Nuclear Research Centre, Boeretang 200, 2400 Mol, Belgium*

[4] *University of Johannesburg, Department of Chemical Engineering, P.O. Box 17011, Doornfontein 2088, South Africa*

GRAPHICAL ABSTRACT

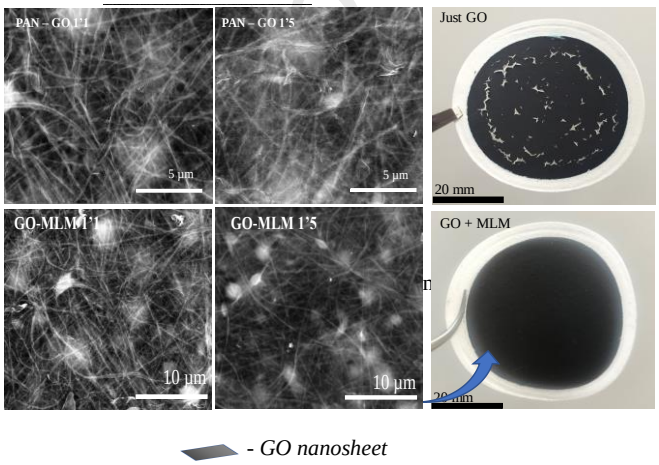

Graphene Oxide Covalent Crosslinking

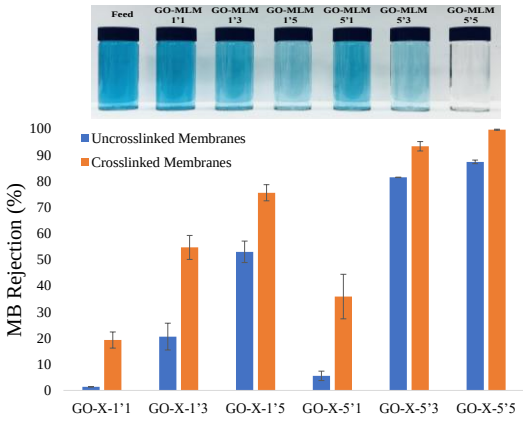

Membrane Performance Improvement with crosslinking

[1]

ABSTRACT

From its physicochemical characteristics, graphene oxide (GO) is a promising versatile next generation membrane material. Its unique characteristics like ultrafast permeation and hydrophilicity makes it a favourable separation membrane nanomaterial in water purification. However, a fundamental problem in the use of GO in nanofiltration is decreased performance overtime due to the pore size widening phenomenon. This paper explored the use of an amine group containing compound, 1,3,5 triazine, 2,4,6 triamine (melamine) to covalently interlink the GO nanosheets to counteract this swelling phenomenon. Prior to membrane fabrication, covalent interactions between GO and the crosslinker, melamine were successfully confirmed through thermogravimetric analysis (TGA), x-ray photoelectron spectroscopy (XPS), X-ray Diffraction (XRD) and Fourier Transform Infra-Red (FTIR) spectroscopy characterisations. Following these characterisations, crosslinked membranes were successfully fabricated and enhanced nanofiltration performance was confirmed. Resultantly, the surface morphology of the membranes was recorded via Scanning Electron Microscopy (SEM) characterisations while a lab-scale nanofiltration device was constructed for flux and rejection analysis. Evidently, performance improvement with covalent crosslinking was imminent as a up to a 100% rejection of methylene blue was achieved for the crosslinked membranes. Structural integrity of GO membranes has indeed been improved through crosslinking.

Keywords: Graphene oxide, crosslinking, melamine, water purification, improvement

[1] Corresponding Author Email: kandjouv@biust.ac.bw, Tel: +267 74 766 991

1.0 Introduction

The exponential increase in global human population and changing climate has heightened the demand for clean water [1–4]. It has been reported that by the year 2050 up to a third of the global human population is likely to experience inaccessibility to clean water [5]. This points to the need for improved and advanced water purification, treatment and desalination means [6–8].

Different water purification and desalination methods thus ought to be developed and improved in efficiency and durability. The methods include conventional ones like distillation, filtration and chemical oriented processes like flocculation and coagulation [9,10]. The use of the latter chemical methods are however impeded by cost intensiveness from large sludge generation and removal post purification as well as damage to separation modules by the chemical species used [11,12]. However, in spite of their wide usage physical methods like distillation are demerited by higher energy consumption which augments operation costs [13].

Separation membranes are continually being favoured over other purification processes [14–16]. This is fostered by their environmental benignity and efficiency in energy conservation. [17]. Several materials from polymeric to inorganic have been and continue to be used in an attempt to have viable and high performing membranes [18,19]. Among the commonly used polymers include poly (vinylidene fluoride) (PVDF), polyacrylonitrile and poly (ethersulfone) [16–19]. Increasingly nonetheless, carbon-based materials are gaining favourability over polymers, the main reason being higher mechanical strength at low density. [24].

The carbon based materials gaining momentum include carbon nanotubes which offer an ultra-fast unidirectional transport of water molecules from the non-slip flow phenomenon [25–27]. However, their poor processability and inability to disperse in solvents as well as complexity in vertical alignment greatly limit progress in their use as separation membranes [28,29]. A promising next generation carbon based material is graphene, owing to exceptional physico-mechanical characteristics [30–33]. Its characteristics gives the prospect of fabricating not only mechanically strong membranes but also thin membranes with a high flux potential. A main hindrance in the use of graphene however has been lack of a cost-effective large scale production method [34,35].

In spite, its oxide form, graphene oxide (GO) is emerging as a significant alternative especially in separation membranes [36,37]. A significance of GO is its ability to be fabricated economically in large scale using several facile methods including the Modified Hummers method [38]. Physico-chemically, GO is a chemically active substance, hydrophilic and 2-dimentional, which makes it an excellent candidate as a separation membrane [39]. Given the fact that the use of GO is still in its primary stage of research, separation mechanisms and emerging challenges ought to be studied more.

Nonetheless, despite the promise, a significant challenge in the use of GO has been outlined by several researchers as decreased nanofiltration performance overtime. This is as a result the accretion of water molecules onto the hydrophilic GO functional groups [40–42], which widens the membrane pores resulting in poor performance. It is therefore of high significance to mitigate this pore-gap widening problem in GO and related membranes to enhance their performance in nanofiltration.

Various means to alleviate the pore-gap widening problem have been and are currently being undertaken. For example, Huang *et al*. studied how removing some of the oxygenated functional which entrap water molecules in GO through chemical reduction impact the performance of the membranes [43]. Despite the improvement in rejection rate, loss of membrane hydrophilicity resulted in reduced flux limiting the efficiency of the membranes [44,45]. Again, Abraham et al. tried to alleviate the pore gap widening problem through nanosheet physical confinement via epoxy encapsulation [46]. However, scaling up this physical confinement method has proven to be a challenge. [46].

In this regard, this paper analyses the use of 1,3,5 triazine 2,4,6 triamine, (melamine), an amine group containing crosslinker to covalently interconnect GO nanosheets to have a stable and mechanically strong crosslinked membrane. The method employed to fabricate the membranes in this paper is the layer-by-layer assembly which offers controlled membrane thickness and enhanced interconnection between the crosslinkers and the GO nanosheets. The method has a potential of giving hybrid membranes with enhanced performance and stability during operation [47], increased membrane intactness henceforth increased membrane durability. Most importantly, the employed crosslinker, melamine is readily available and affordable in most regions of the world.

2.0 Experimental Section

2.0.1 Materials

GO powder was commercially sourced from Graphenea (Spain). Fibrous Polyacrylonitrile (PAN) support substrates acquired from Whatman; UK were used as the base structure for the membranes. The crosslinker, 1,3,5 triazine 2,4,6 triamine (melamine) (MLM) (product code: M2659) and Polyethyleneimine (PEI) (product code 03880) which was used during substrate pre-treatment, were purchased from Sigma-Aldrich (UK). Prior to membrane fabrication, the substrates were activated using a 1M solution of Potassium hydroxide (KOH). The nanofiltration performance of the membranes on the other hand was carried out using methylene blue (MB) as the contaminant. All these were again purchased from Sigma Aldrich, UK

.2.0.2 Membrane Fabrication

2.0.2.1 Polyacrylonitile (PAN) substrate Pre-treatment

Owing to the presence of acrylonitrile groups (-C≡N) in PAN, there are several ways in which this substrate can be pre-treated and modified to facilitate interaction with other species. Among commonly used methods are plasma-initiated graft polymerisation [48,49], photo-induced grafting and hydrolysis [50–52].

To pre-treat the membrane supporting PAN substrates, they were first immersed in a KOH solution for 30 minutes at 70 ℃. KOH instigated the formation of carboxylate function groups, which are electrostatically negatively charged [53–55]. The now negatively charged substrates were then excessively rinsed with distilled water. This is followed by putting them in a positively charged solution of PEI to confer a positive charge [53,55] making the substrates ready for membrane assembly..

2.0.2.2 Control and MLM crosslinked membrane fabrication

The membranes were fabricated with an automated rotary dip-coater (Nadetech Innovations, Navarra, Spain). The layer-by-layer fabrication time and the number of dips were set at 1 and 5 minutes and 1, 3 and 5 respectively with the assistance of an ND-R Rotatory Coater Software. They were then labelled accordingly to show the immersion time and assembly cycles, for instance crosslinked membranes fabricated under 1 minute immersion time for 5 assembly cycles was duly labelled GO-MLM 1'5.

A 0.5 mg/ml water suspension of GO was used as it was noted by the manufacturer, Graphenea that at this concentration there is fewer agglomeration of the nanosheets. The suspension was then sonicated for 2 hours to hasten the individuality and stability of the suspension prior to fabrication. The control, uncrosslinked where just dip-coated while for the crosslinked membranes were fabricated using the dip-assisted layer by layer method, alike in our previous studies [56–59]. Here, an interchangeable immersion between GO and MLM is undertaken in order to interconnect the GO nanosheets and the crosslinker.

2.0.3 Membrane Nanofiltration Tests

To compare the nanofiltration performance of the fabricated membranes, a methyl methacrylate homemade nanofiltration cell alike in our previous works [58] was constructed. In this cell a porous sintered polyethylene plate with a 4.7 cm diameter was used. It was water-tightened by neoprene gaskets and the driving force used to push the 'wastewaters' across the membranes was nitrogen gas at 1 bar.

1L of 10 mg/L of a solution of methylene blue was used as the feed solution. The parameter to establish the differences in performance here was permeation flux, calculated by the equation below, and the rejection rate.

142 $F = \frac{V}{At}$ Equ (1)

143 Where the flux is represented by F, A, the membrane operation effective area and t, the nanofiltration time
144 taken.

145 To determine the rejection rate of the membranes, Ultra-Violet -Visible Light characterisations of the feed
146 and permeate solutions were undertaken. A calibration line following the Lambert-Bear law application
147 linear range was constructed to calculate a concentration-based membrane rejection rate.

148 Separation rejection [R (%)] was subsequently determined using the equation below in which C_p and C_f are
149 the permeate and feed concentrations respectively.

150 $R(\%)=\left(1-\frac{Cp}{Cf}\right)\times 100$ Equ (2)

151 The dependability and accuracy of the rejection and permeation flux results was heightened by taking an
152 average of four membrane tests and the standard deviation was accordingly noted.

153 2.0.4 Continuity of the fabricated membranes

154 The sound structure and surface continuity of the fabricated membranes is significant in the efficiency and
155 performance of the membranes. Membrane structure before and after nanofiltration was determined by a
156 JEOL JSM – 5900 SEM. This was done to verify the maintenance of membrane intactness with
157 crosslinking.

158 2.0.5 Pre-membrane Fabrication Characterisations

159 Before membrane fabrication, GO suspensions and the solution of the crosslinker, MLM were reacted
160 together to verify the nature and plausible interaction between the two membrane constituents. Fourier
161 Transform Infra-Red (Attenuated total reflectance unit (ATR)-PerkinElmer Spectrometer), X-ray
162 Photospectroscopy [Kratos Ultra-DLD XPS System (K-Alpha+)] and Thermogravimetric
163 Analysis (SF) (METTLER-TOLEDO) characterisations were undertaken to verify and confirm
164 interaction between GO and the crosslinker. The inter-flake gap of GO nanosheets and GO-MLM
165 reacted sample was evaluated via XRD characterizations using a Thermo Scientific ARL XTRA
166 Powder Diffractometer which features a copper X-ray tube and a goniometer system providing
167 resolution in the low angle region, CuKα radiation (λ=1.5418 A). The interflake gap of the
168 prepared samples was calculated using the Bragg equation (Equation 3).

$$2dSin(\theta) = n\lambda. \quad \text{Eq (3)}$$

Where d: the inter nanosheet gap,θ: the XRD angle λ is the wavelength of the x-ray and n is an integer (order of reflection).

3.0 Results and Discussion

3.0.1 Confirmation of Covalent Interaction between GO and Melamine

It was significant to demonstrate and proof the form of interaction facilitating the connection between GO and melamine (MLM) before membrane fabrication. Hybridisation of GO membranes by the crosslinker is necessary for forming stable crosslinked GO membranes [60]. Consequently, respective characterisations like FTIR TGA, DTG and XPS characterization results confirmed GO-melamine covalent interactions. And this lays the possibility of crosslinking GO based membranes using melamine.

From the FTIR characterisations, the structural chemistry of GO at hand was verified by confirming functional groups present in GO (Figure 1). For instance, at 3340 cm^{-1}, a dip advocated to the hydroxyl (-O-H) is observed. Other present groups in GO such as the ketone (-C=O), carboxylic and ester groups are represented by the band at 1726 cm^{-1} [61–65], while bands observed at around 1616 cm^{-1} and 1016 cm^{-1} are advocated to the C=C vibrations and the epoxide groups respectively [66].

The most significant functional group to substantiate the interaction between melamine and GO are the amine groups. The presence of these primary amine groups in FTIR characterisations are indicated by three bands between 3400 cm^{-1} and 3000 cm^{-1} [67–69] (Figure 1). The dip observed at around 3460 cm^{-1} represent the -N-H symmetric stretching present in melamine [70]. The subsequent bands observed at 1630 cm^{-1} and 1506 cm^{-1} are advocated to the deforming vibrations of the -N-H groups also present in MLM [71,72]. The triazine ring is on the other hand represented by the 1418 cm^{-1} band (Figure 1) [73].

From the GO-MLM spectra, the disappearance of the characteristic primary amine three bands observed in the 3400-3000 cm^{-1} area is notable in the reacted entities (Figure 1). This suggest the generation of secondary amines following MLM-GO reaction [69], moreover a clear peak at 1510 cm^{-1} is present, indicating the presence of an -N-H secondary group [69,72]. This is due to the chemical reaction between the epoxy group in GO and amines in MLM (see schematic 1).

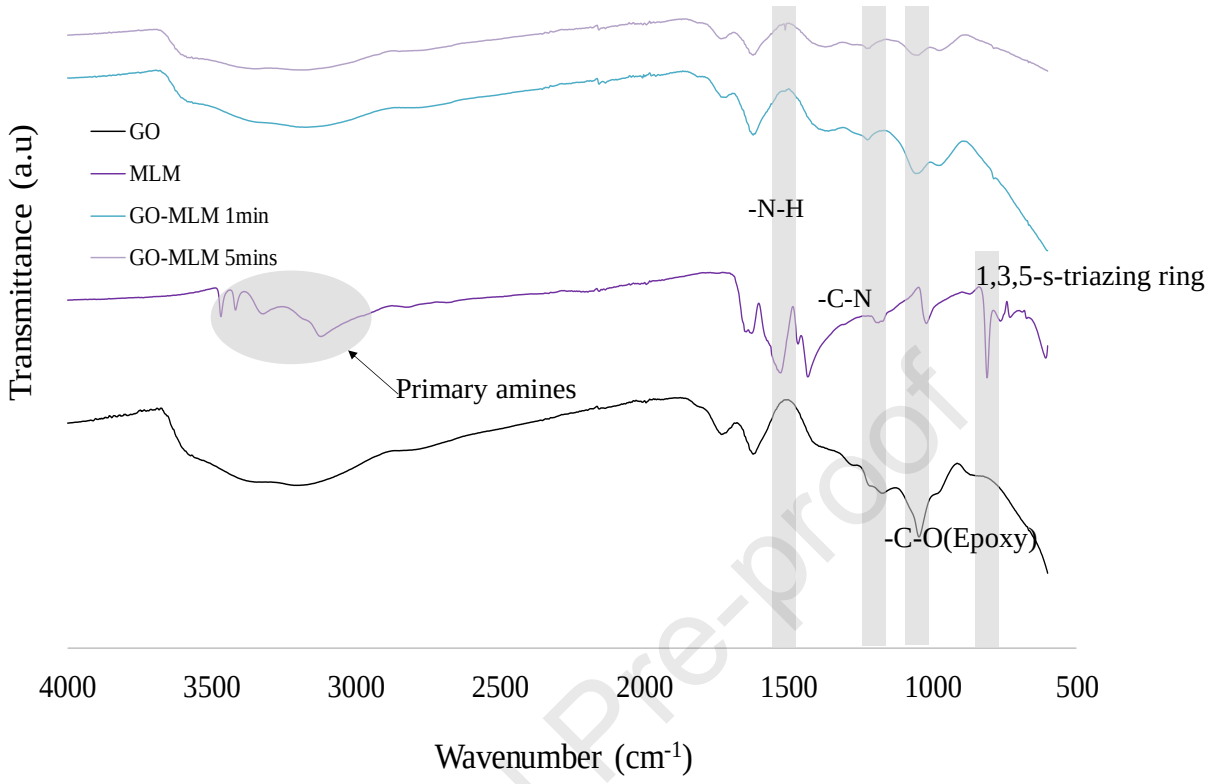

Figure 1. *FTIR spectra of GO, MLM and GO-MLM hybrid at respective reaction times*

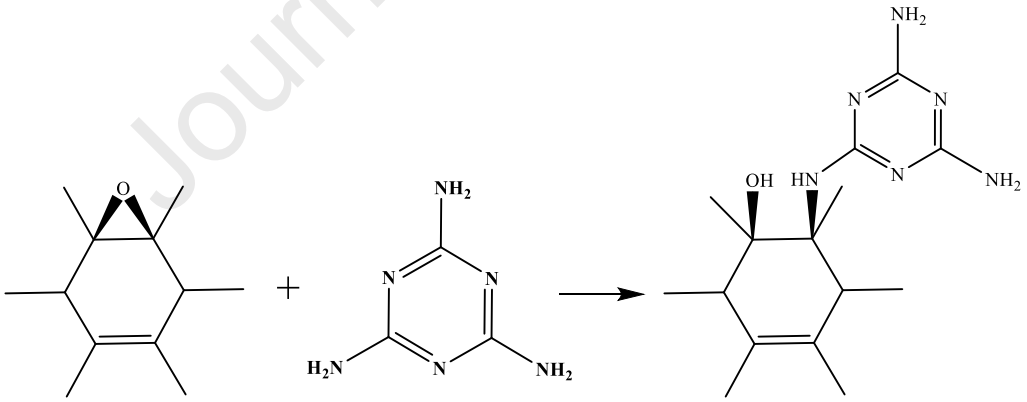

Scheme 1. *GO-MLM predominant interaction between GO and Melamine*

The epoxy-ring-opening reaction between MLM and GO is also backed by the diminishment of the epoxide band at 1060 cm^{-1} in the GO FTIR spectrum [66]. The observed FTIR results are in consonance with the XPS characterisations observed in Figure 2 and Table 1. From the XPS characterisations, reduction in the

epoxy prevalence in the MLM-GO reacted entities are notable (Table 1). Moreover, the generation of a -C-N band validated by an increase in the prevalence of the C-N covalent band from 1.2% to about 15% in these XPS characterisations further confirms a covalent interaction between GO and MLM.

It is expected that an amide linkage will be formed from the interaction of carboxylic groups in GO and the amines in MLM, however no evidence attesting to this was observed. However, given the fabrication conditions entailed, the reaction between amines and carboxylic acid groups is highly unlikely under aqueous conditions in the absence of catalysts and coupling compounds [74]. In this reaction types, acid-activation chemistry is required to instigate such reactions [75]; nonetheless a competitive reaction with active nucleophiles in water do occur. The epoxy ring opening reaction is thus the predominant mode of interaction in this regard as observed elsewhere [76,77].

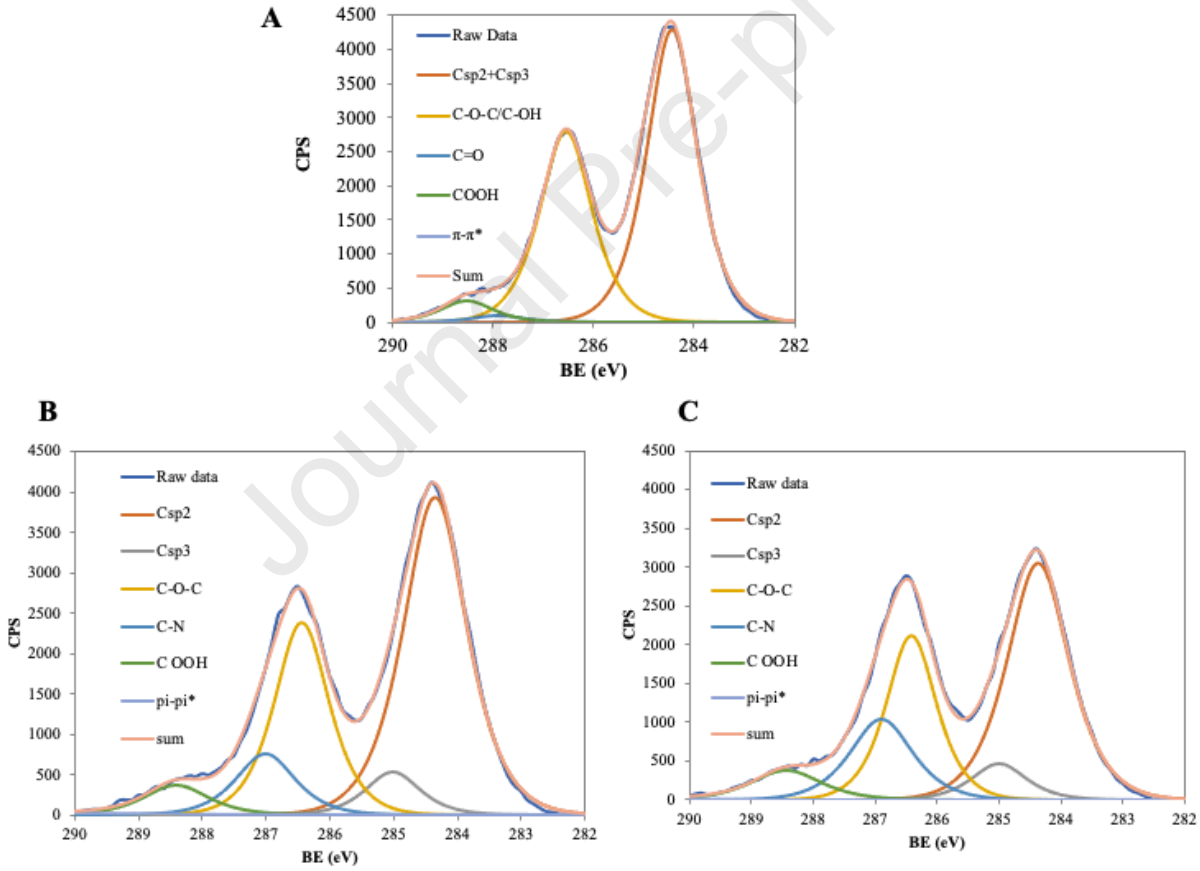

Figure 2. A; GO, B: GO-MLM 1 minute and GO-MLM 5 minutes XPS spectra.

Table 1. *XPS Characterisations of GO and GO-MLM reacted entities.*

	GO	GO-MLM reacted 1 min	GO-MLM reacted 5min
C1s (%)	71.2	68.2	68.4
O1s (%)	27.4	31.0	30.9
S1s (%)	1.4	0.0	0.0
N1s (%)	---	0.8	0.7
$Csp^2 + Csp^3$(%)	58.5	47.6	48.9
C(epoxy)/C=N (%)	37.1	34.5	32.5
C=O/C-N (%)	1.2	13.0	16.1
COOH (%)	3.2	4.6	2.2
π-π* (%)	0.0	0.3	0.3

It can further be noted that the presence of various functional groups in GO and the crosslinker is likely to cause non-covalent interactions like hydrogen bonding and van der Waals' forces, [78] as noted in related works [79,80]. π – π interactions between the non-oxidised region in GO and the triazine region in MLM are also highly plausible [80,81].

Further confirmation of covalent interaction between MLM and GO was confirmed by DTG and TGA analysis. The reacted entities shows that the complete decomposition temperature of pure GO in improved by about 50^{o}C and an enhancement in weight-loss temperature is also notable with crosslinking (Figure 3). This shows a significant improvement in thermos-oxidative stability of pure GO which is tantamount to an increase structural integrity of the resultant hybrid membrane material. [82]. This suggests that the epoxide groups are converted to the more stable covalent -C-N bonds as aforementioned, culminating in improved thermal stability [82,83]. The DTG and TGA analysis results are thus in consonance with the FTIR and XPS characterisations, further confirming covalent interaction between GO and the MLM crosslinker.

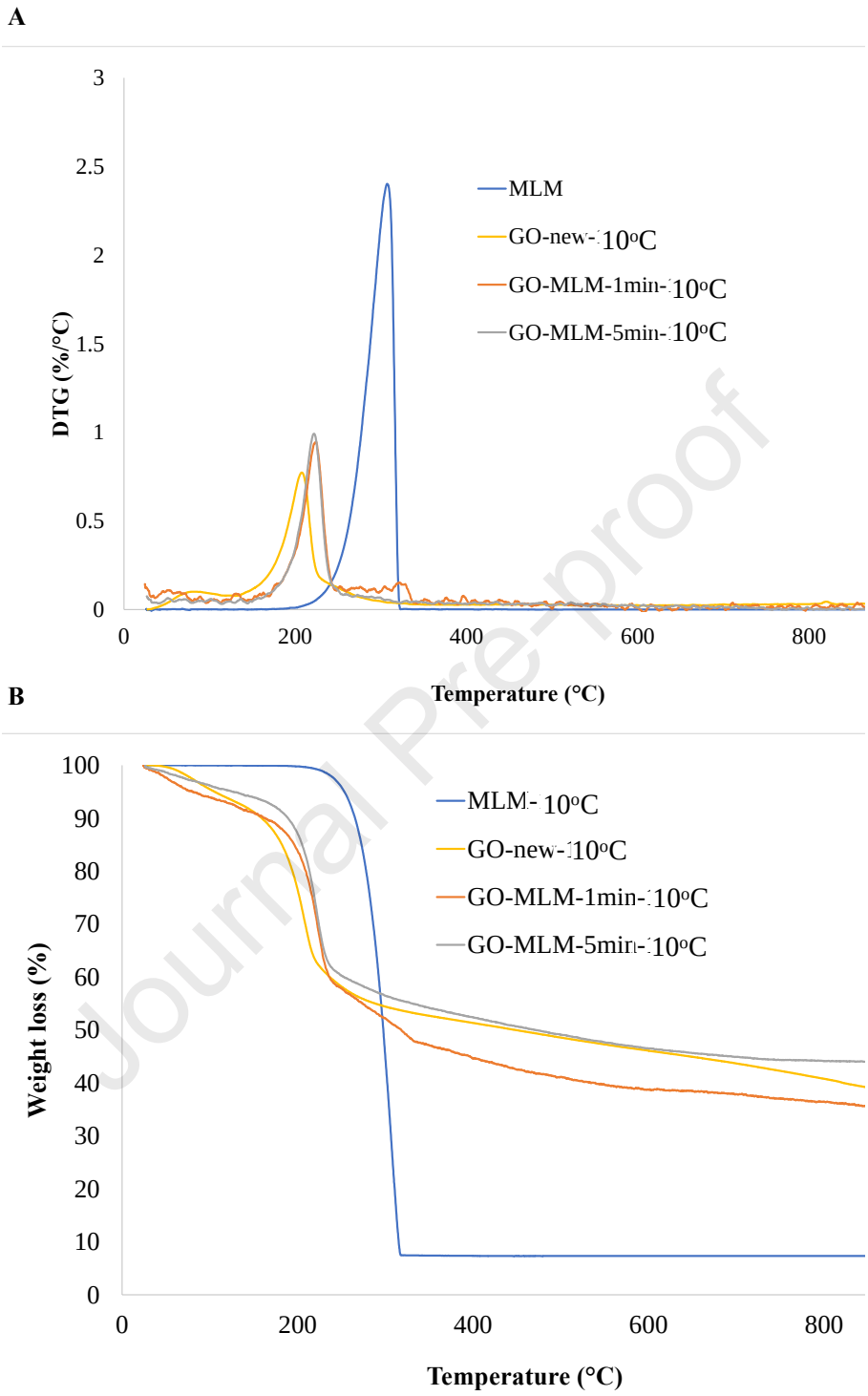

234

235 ***Figure 3**: A) DTG and B) TGA analysis of the GO, MLM and GO-MLM hybrid mixture*

3.0.2 Membrane Surface Coverage

The fabricated crosslinked and uncrosslinked membranes at the respective fabrication time and bi-layers are shown in Figure 4. The uncrosslinked and MLM crosslinked membranes are labelled accordingly, for instance GO-1'1 being the uncrosslinked membranes fabricated under 1 minute immersion time at 1 layer. It can be observed there is an augmentation in the darkening of the colour of the membranes with an increase in number of membrane assembly cycles and immersion time. Good continuity coverage and homogeneity is also visible as duly confirmed by SEM characterisations (Figure 5). Continuity coverage for the uncrosslinked membranes is supported by the non-covalent connections between the GO functional groups [84], while the proven covalent interaction facilitates the GO-MLM interactions in the crosslinked membranes [60,85]. Subsequent SEM characterisations confirms the continuity coverage of these membranes. The plain PAN substrates are also shown in the respective images to show continuity coverage.

Figure 4. *Images of the fabricated membranes*

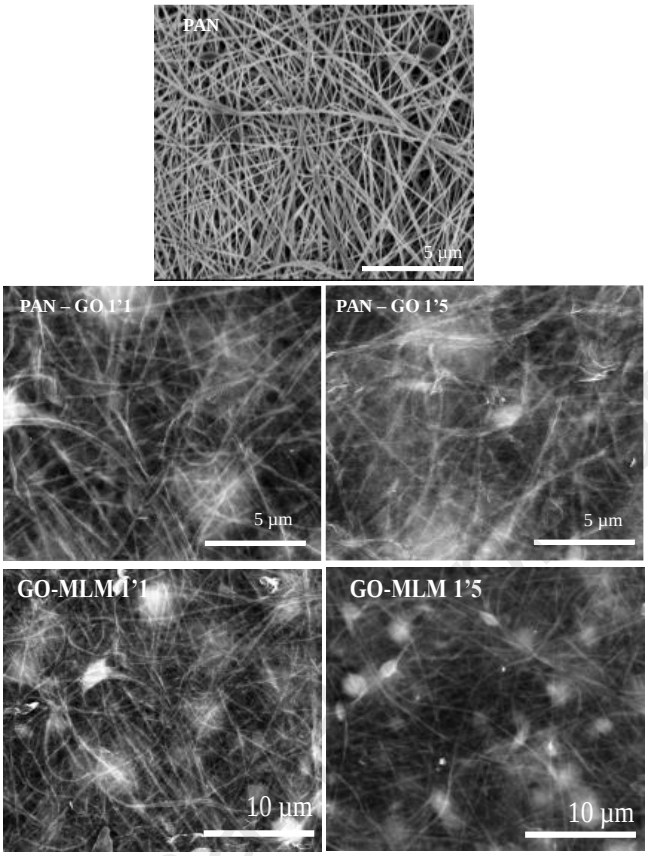

Figure 5. *SEM of plain PAN substrates, uncrosslinked and crosslinked membranes*

3.0.3 Membranes Nanofiltration Results

3.0.3.1 Rejection analysis

The main aim of the paper as was to improve the performance of GO membranes in nanofiltration through crosslinking with melamine. Evidently a comparison of the nanofiltration performance of the fabricated membranes' dye retention shows an improvement in membrane nanofiltration with crosslinking. Lessening in colouration with increased membrane rejection is evident. This was further proven by the UV-Vis characterization average rejection results shown in figure 7.

The characterisations show that at equivalent membrane fabrication conditions, the crosslinked membranes had a better dye rejection. For instance, the MLM crosslinked membranes fabricated under 5-minutes dipping time, experienced a dye retention rate increase from 35.9 % to 99.7 % as the bi-layers increased from 1 to 5. Relatively, the rejection rate for the control membranes also increased with number of layers but at a lower rate (Figure 7), signifying a notable improvement in performance with crosslinking. This

notable difference is advocated to poor stability of the uncrosslinked membranes during nanofiltration, instigated by the widening of the membrane pore gap [40,41].

The crosslinked membranes showed a relatively smaller pore size of 0.80278 nm in comparison to the uncrosslinked membranes with a relative pore-size measured at 0.86398 nm (figure 6). The observed difference is mostly due to the covalent interaction between GO and the crosslinker and this is likely to maintain the pore-gap even during nanofiltration for the crosslinked membranes stemming from the strength of the –C-N covalent bond [86]. Hence the observed improvement in performance with crosslinking.

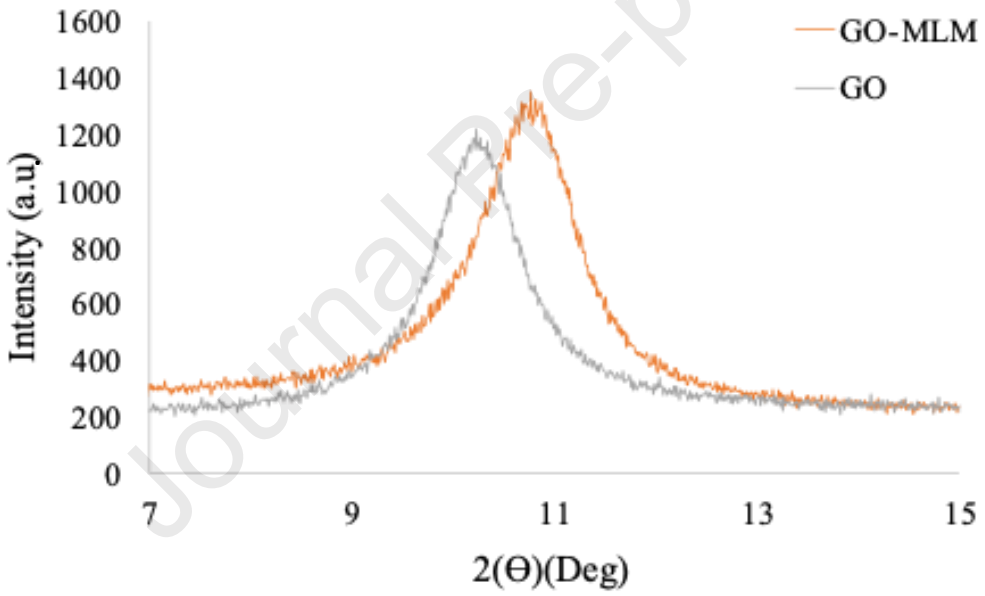

Figure 6: XRD Characterisations of crosslinked and uncrosslinked membranes

The significance of crosslinking with a covalent sub-nanometre sized MLM compounds is in this instance validated.

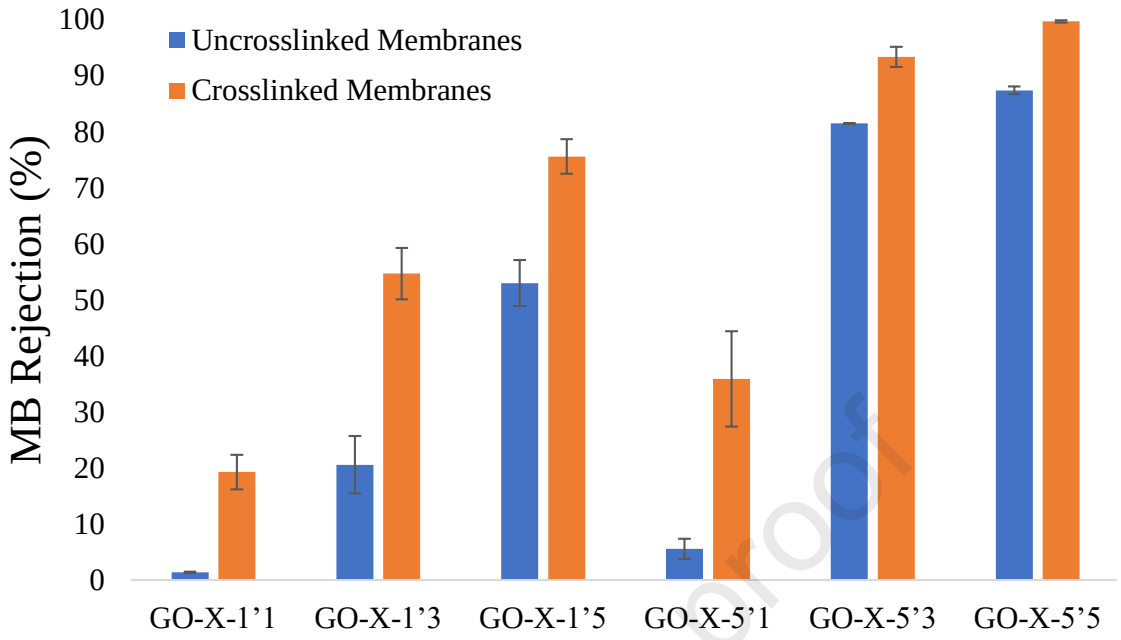

Figure 7. *Histograms of membrane MB rejection tests*

It can be argued that improvement in performance with crosslinking, indicates that the crosslinkers improves the integrity of the GO matrix through the confirmed covalent C-N bonds.

3.0.3.2 Permeation Flux Results

In consonance with the MB retention results observed, the flux decreases with an augmentation in the number of assembly cycles as well as the immersion time. An increase in immersion time and bi-layers culminates in the increase of the water flow-path of the membranes [87,88]. Crosslinking comes with decrease in flux as a result of confinement of the pores of the membranes by the crosslinker. This trend is observable when comparing the crosslinked and uncrosslinked membranes at similar fabrication conditions (Figure 8).

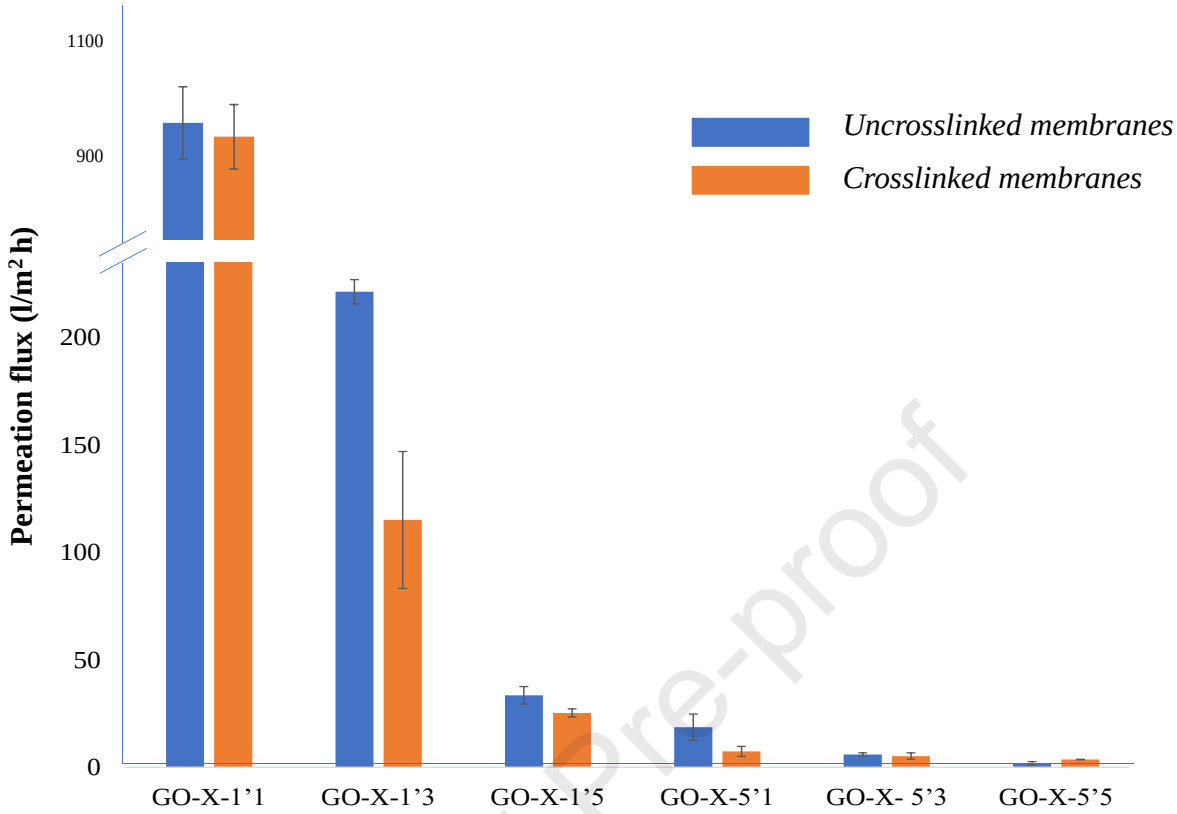

287

288 ***Figure 8.*** *Flux of the respective membranes (Crosslinked and Uncrosslinked)*

289

290 Despite the relatively recorded low fluxes at increased materials accumulation, there is a notable
291 improvement when comparing with related works in literature. For instance, a flux rate ranging from 0.58
292 l/m^2.h to 0.60 l/m^2.h has been reported in the separation of methylene blue using a high driving pressure of
293 up to 15 bars [89]. The performance of the modified membranes here is thus imperative. The membranes
294 are also applicable in the separation of other common contaminants and even heavy metals subject to
295 relevant modifications.

296 3.0.4 Membrane stability

297 Post operation membrane, characterization to determine the stability, re-usability and operation longevity
298 of the membranes were undertaken. SEM imaging was done again to verify the maintenance of intactness
299 for both membrane types.

300 From the SEM characterisations, micrometre-sized cracks are visible in the uncrosslinked membranes post
301 nanofiltration (Figure 9) The cracks are likely a result of nanosheet shrinkage during drying. [90]. On the

contrary for the MLM crosslinked membranes, intactness is maintained owing to the covalent holding together of the GO nanosheets by melamine via the C-N bond and other non-covalent interactions.

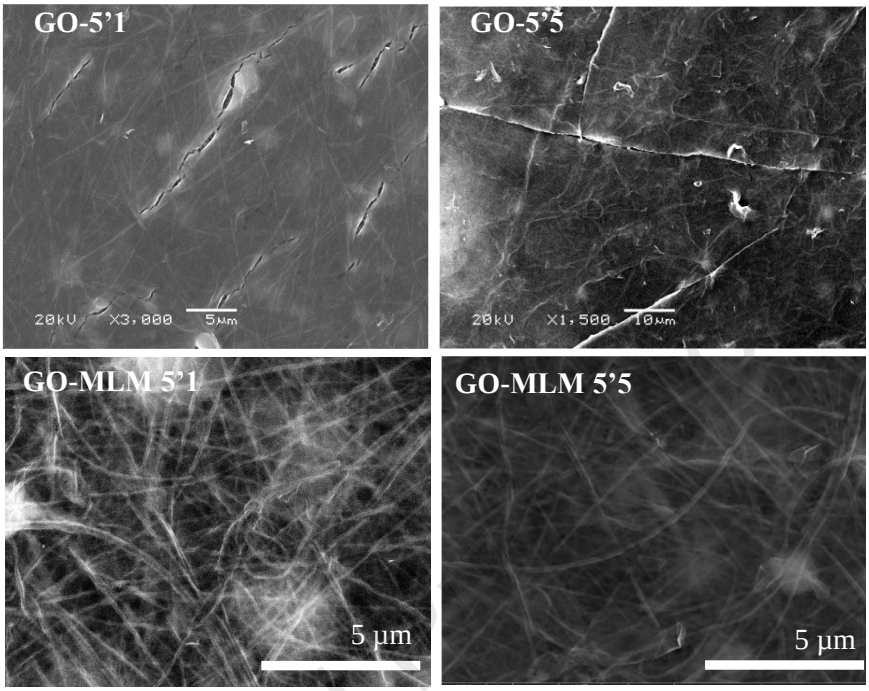

Figure 91. *SEM images of the respective membranes after nanofiltration.*

4.0 Conclusions

In summation, the significance of covalent crosslinking of GO membranes has been successfully demonstrated. The importance of crosslinking is clearly evident with up to 100% separation of the MB contaminant achieved. The crosslinker in this case is not only significant in improving the nanofiltration performance of the membranes but also instigating the integrity of the membranes. This guarantees membrane durability and operation longevity. The work thus offers other potential applications of these crosslinked membranes subject to relevant modifications for the intended applications.

5.0 Acknowledgment

The authors would like so to send sincere regards to the Botswana Government for offering the Top-Achievers Scholarship (TR-100159844RA3-163096) that facilitated this work. Special thanks also go to the HarwellXPS National Facility (Cardiff, UK) as well as the Carbon Science and Technology Institute (INCAR-CISC) in Oviedo, Spain for aiding with XPS and TGA characterizations respectively.

6.0 References

[1] M. Kummu, J.H.A. Guillaume, H. De Moel, S. Eisner, M. Flörke, M. Porkka, The world ' s road to water scarcity : shortage and stress in the 20th century and pathways towards sustainability, Nat. Publ. Gr. (2016) 1–16. https://doi.org/10.1038/srep38495.

[2] R.I. Mcdonald, P. Green, D. Balk, B.M. Fekete, C. Revenga, M. Todd, freshwater availability, 108 (2011) 6312–6317. https://doi.org/10.1073/pnas.1011615108.

[3] S.J. Mcgrane, Impacts of urbanisation on hydrological and water quality dynamics , and urban water management : a review water management : a review, Hydrol. Sci. J. 61 (2016) 2295–2311. https://doi.org/10.1080/02626667.2015.1128084.

[4] V. Srinivasan, E.F. Lambin, S.M. Gorelick, B.H. Thompson, S. Rozelle, The nature and causes of the global water crisis : Syndromes from a meta-analysis of coupled human-water studies, 48 (2012) 1–16. https://doi.org/10.1029/2011WR011087.

[5] W. World Health Organization, Meeting the MDG drinking water and sanitation, the urban and rural challenge of the decade, Geneva, 2007. http://www.who.int/water_sanitation_health/monitoring/jmpfinal.pdf.

[6] K. Balke, Y. Zhu, Natural water purification and water management by artificial groundwater recharge, J. Zhejiang Univ. Sci. B. 9 (2008) 221–226. https://doi.org/10.1631/jzus.B0710635.

[7] M. Shatat, S.B. Riffat, Water desalination technologies utilizing conventional and renewable energy sources, (2014) 1–19. https://doi.org/10.1093/ijlct/cts025.

[8] M. Elimelech, W.A. Phillip, The Future of Seawater Desalination: Energy, Technology and the Environment, Science (80-.). 333 (2011) 712–718. https://doi.org/10.1126/science.1200488.

[9] A. Grumezescu, Water Purification (Nanotechnology in the Agri-Food Industry), 2nd ed., Academic Press, 2017, London, 2017. https://www.abebooks.com/9780128043004/Water-Purification-Nanotechnology-Agri-Food-Industry-0128043008/plp.

[10] V. Kandjou, D.O. Nkwe, F. Ntuli, N. Keroletswe, Evaluating the degree of chemical contamination of underground aquifers in Botswana and analysing viable purification and desalination means; a review, Chem. Eng. Res. Des. (2022). https://doi.org/https://doi.org/10.1016/j.cherd.2022.03.055.

[11] S. Bolisetty, M. Peydayesh, R. Mezzenga, Sustainable technologies for water purification from

heavy metals: review and analysis, Chem. Soc. Rev. 48 (2019) 463–487. https://doi.org/10.1039/c8cs00493e.

[12] M. Al-Abri, B. Al-Ghafri, T. Bora, S. Dobretsov, J. Dutta, S. Castelletto, L. Rosa, A. Boretti, Chlorination disadvantages and alternative routes for biofouling control in reverse osmosis desalination, Npj Clean Water. 2 (2019). https://doi.org/10.1038/s41545-018-0024-8.

[13] S. Sharma, A. Bhattacharya, Drinking water contamination and treatment techniques, Appl. Water Sci. 7 (2017) 1043–1067. https://doi.org/10.1007/s13201-016-0455-7.

[14] P. Bernardo, G. Clarizia, 30 Years of Membrane Technology for Gas Separation, 32 (2013) 1999–2004.

[15] S. Heinrich, Membranes and Membrane Separation Processes, 1st ed., Wiley-VCH, 2005. https://onlinelibrary.wiley.com/doi/abs/10.1002/14356007.a16_187.pub2.

[16] S. LOEB, S. SRINIVASA, Sea Water Demineralization by Means of an Osmotic Membrane, in: 2nd ed., American Chemical Society, Calif, 1963: pp. 117–132. https://doi.org/10.1021/ba-1963-0038.ch009.

[17] Z. Wang, A. Wu, Recent Advances in Nanoporous Membranes for Water Purification, Nanomaterials. 9 (2018). https://doi.org/10.3390/nano8020065.

[18] E.. Mason, From pig bladders and cracked jars to polysulfones: An historical perspective on membrane transport, J. Memb. Sci. 20 (1991) 125–145. https://doi.org/10.1016/S0376-7388(00)81529-X.

[19] W.. Koros, M.. Hellums, Gas separation membrane material selection criteria: Differences for weakly and strongly interacting feed components, Fluid Phase Equilib. 53 (1989) 339–354. https://doi.org/10.1016/0378-3812(89)80102-5.

[20] Y. Yampolskii, Polymeric Gas Separation Membranes, Macromolecules. 45 (2012) 3298–3311. https://doi.org/10.1021/ma300213b.

[21] L.M. Robeson, Polymer membranes for gas separation, Curr. Opin. Solid State Mater. Sci. 4 (2000) 549–552.

[22] G.M. Geise, H. Lee, D.J. Miller, B.D. Freeman, J.E. Mcgrath, D.R. Paul, H. Lee, D.J. Miller, Water Purification by Membranes : The Role of Polymer Science, J. Polym. Sci. Part B Polym. Phys. 48 (2010) 1685–1718. https://doi.org/10.1002/POLB.

[23] H. Ma, C. Burger, B.S. Hsiao, B. Chu, Highly Permeable Polymer Membranes Containing Directed Channels for Water Purification, ACS Macroletters. 1 (2012) 723–726. https://doi.org/10.1021/mz300163h.

[24] C.A.. Siskens, Chapter 13 Applications of ceramic membranes in liquid filtration, Membr. Sci. Technol. 4 (1996) 619–639. https://www.sciencedirect.com/science/article/abs/pii/S0927519396800167.

[25] A. Kalra, S. Garde, G. Hummer, Osmotic water transport through carbon nanotube membranes, Proc. Natl. Acad. Sci. U. S. A. 100 (2003) 10175–10180. https://doi.org/10.1073/pnas.1633354100.

[26] J.K. Holt, H.G. Park, Y. Wang, M. Stadermann, A.B. Artyukhin, C.P. Grigoropoulos, A. Noy, O. Bakajin, Fast Mass Transport Through Sub – 2-Nanometer Carbon Nanotubes, Science (80-.). 312 (2006) 1034–1038. https://doi.org/10.1126/science.1126298.

[27] M. Majumder, N. Chopra, B.J. Hinds, Mass transport through carbon nanotube membranes in three different regimes: Ionic diffusion and gas and liquid flow, ACS Nano. 5 (2011) 3867–3877. https://doi.org/10.1021/nn200222g.

[28] M. Yu, H.H. Funke, J.L. Falconer, R.D. Noble, High Density, Vertically-Aligned Carbon Nanotube Membranes, Nano Lett. 9 (2009) 225–229. https://doi.org/10.1021/nl802816h.

[29] S. Kim, J.R. Jinschek, H. Chen, D.S. Sholl, E. Marand, Scalable fabrication of carbon nanotube/polymer nanocomposite membranes for high flux gas transport, Nano Lett. 7 (2007) 2806–2811. https://doi.org/10.1021/nl071414u.

[30] N. Song, X. Gao, Z. Ma, X. Wang, Y. Wei, C. Gao, A review of graphene-based separation membrane : Materials, characteristics, preparation and applications, Desalination. 437 (2018) 59–72. https://doi.org/10.1016/j.desal.2018.02.024.

[31] P. Liu, T. Yan, J. Zhang, L. Shi, D. Zhang, Separation and recovery of heavy metal ions and salt ions from wastewater by 3D graphene-based asymmetric electrodes via capacitive deionization, J. Mater. Chem. A. 5 (2017) 14748–14757. https://doi.org/10.1039/c7ta03515b.

[32] R.P. Pandey, G. Shukla, M. Manohar, V.K. Shahi, Graphene oxide based nanohybrid proton exchange membranes for fuel cell applications : An overview, Adv. Colloid Interface Sci. 240 (2017) 15–30. https://doi.org/10.1016/j.cis.2016.12.003.

[33] R.I. Jafri, N. Rajalakshmi, S. Ramaprabhu, Nitrogen doped graphene nanoplatelets as catalyst

support for oxygen reduction reaction in proton exchange membrane fuel cell, J. Mater. Chem. 20 (2010) 7114–7117. https://doi.org/10.1039/c0jm00467g.

[34] A. Zurutuza, C. Marinelli, Challenges and opportunities in graphene commercialization, Nat. Nanotechnol. 9 (2014) 730–734. https://doi.org/10.1038/nnano.2014.225.

[35] L. Dong, J. Yang, M. Chhowalla, K.P. Loh, Synthesis and reduction of large sized graphene oxide sheets, Chem. Soc. Rev. 46 (2017) 7306–7316. https://doi.org/10.1039/c7cs00485k.

[36] R.K. Joshi, S. Alwarappan, M. Yoshimura, V. Sahajwalla, Y. Nishina, Graphene oxide: The new membrane material, Appl. Mater. Today. 1 (2015) 1–12. https://doi.org/10.1016/j.apmt.2015.06.002.

[37] R.K. Joshi, P. Carbone, F.C. Wang, V.G. Kravets, Y. Su, I.. Grigorieva, H.. Wu, A.K. Geim, R.R. Nair, Precise and Ultrafast Molecular Sieving Through Graphene Oxide Membranes, Science (80-.). 343 (2014) 752–755. https://doi.org/10.1126/science.1245711.

[38] W.S. Hummers, R.E. Offeman, Preparation of Graphitic Oxide, J. Am. Chem. Soc. 80 (1958) 1339. https://doi.org/10.1021/ja01539a017.

[39] R.. Nair, H.. Wu, A. V. Jayaram, V. Grigorieva, A.. Geim, Unimpeded Permeation of Water Through Helium-Leak–Tight Graphene-Based Membranes, Science (80-.). 335 (2012) 442–445. https://doi.org/10.1126/science.1211694.

[40] S. Zheng, Q. Tu, J.J. Urban, S. Li, B. Mi, Swelling of Graphene Oxide Membranes in Aqueous Solution: Characterization of Interlayer Spacing and Insight into Water Transport Mechanisms, ACS Nano. 11 (2017) 6440–6450. https://doi.org/10.1021/acsnano.7b02999.

[41] Y. Mo, X. Zhao, Y. xiao Shen, Cation-dependent structural instability of graphene oxide membranes and its effect on membrane separation performance, Desalination. 399 (2016) 40–46. https://doi.org/10.1016/j.desal.2016.08.012.

[42] I. Chandio, F.A. Janjhi, A.A. Memon, S. Memon, Z. Ali, K.H. Thebo, A.A.A. Pirzado, A.A. Hakro, W.S. Khan, Ultrafast ionic and molecular sieving through graphene oxide based composite membranes, Desalination. 500 (2021) 114848. https://doi.org/10.1016/j.desal.2020.114848.

[43] L. Huang, J. Chen, T. Gao, M. Zhang, Y. Li, L. Dai, L. Qu, G. Shi, Reduced Graphene Oxide Membranes for Ultrafast Organic Solvent Nanofiltration, Adv. Mater. 28 (2016) 8669–8674. https://doi.org/10.1002/adma.201601606.

[44] S. Abdolhosseinzadeh, H. Asgharzadeh, H.S. Kim, Fast and fully-scalable synthesis of reduced graphene oxide, Sci. Rep. 5 (2015) 1–7. https://doi.org/10.1038/srep10160.

[45] M. Omidvar, M. Soltanieh, S.M. Mousavi, E. Saljoughi, A. Moarefian, H. Saffaran, Preparation of hydrophilic nanofiltration membranes for removal of pharmaceuticals from water, J. Environ. Heal. Sci. Eng. 13 (2015) 1–9. https://doi.org/10.1186/s40201-015-0201-3.

[46] J. Abraham, K.S. Vasu, C.D. Williams, K. Gopinadhan, Y. Su, C.T. Cherian, J. Dix, E. Prestat, S.J. Haigh, I. V. Grigorieva, P. Carbone, A.K. Geim, R.R. Nair, Tunable sieving of ions using graphene oxide membranes, Nat. Nanotechnol. 12 (2017) 546–550. https://doi.org/10.1038/nnano.2017.21.

[47] W.S. Hung, C.H. Tsou, M. De Guzman, Q.F. An, Y.L. Liu, Y.M. Zhang, C.C. Hu, K.R. Lee, J.Y. Lai, Cross-linking with diamine monomers to prepare composite graphene oxide-framework membranes with varying d-spacing, Chem. Mater. 26 (2014) 2983–2990. https://doi.org/10.1021/cm5007873.

[48] Z. Zhao, J. Li, D. Zhang, C.-X. Chen, Nanofiltration membrane prepared from polyacrylonitrile ultrafiltration membrane by low-temperature plasma: I. Graft of acrylic acid in gas, J. Memb. Sci. 232 (2004) 1–8. https://doi.org/10.1016/j.memsci.2003.11.009.

[49] Z. Zhao, J. Li, D. Wang, C.-X. Chen, Nanofiltration membrane prepared from polyacrylonitrile ultrafiltration membrane by low-temperature plasma: 4. grafting of N-vinylpyrrolidone in aqueous solution, Desalination. 184 (2005) 37–44. https://doi.org/https://doi.org/10.1016/j.desal.2005.04.036.

[50] G. Zhang, H. Yan, S. Ji, Z. Liu, Self-assembly of polyelectrolyte multilayer pervaporation membranes by a dynamic layer-by-layer technique on a hydrolyzed polyacrylonitrile ultrafiltration membrane, J. Memb. Sci. 292 (2007) 1–8. https://doi.org/10.1016/j.memsci.2006.11.023.

[51] G. Zhang, X. Gao, S. Ji, Z. Liu, Electric field-enhanced assembly of polyelectrolyte composite membranes, J. Memb. Sci. 307 (2008) 151–155. https://doi.org/10.1016/j.memsci.2007.09.030.

[52] X.P. Wang, N. Li, W.Z. Wang, Pervaporation properties of novel alginate composite membranes for dehydration of organic solvents, J. Memb. Sci. 193 (2001) 85–95. https://doi.org/10.1016/S0376-7388(01)00498-7.

[53] Q. Nan, P. Li, B. Cao, Fabrication of positively charged nanofiltration membrane via the layer-by-layer assembly of graphene oxide and polyethylenimine for desalination, Appl. Surf. Sci. 387

(2016) 521–528. https://doi.org/10.1016/j.apsusc.2016.06.150.

[54] O. Sanli, Homogeneous hydrolysis of polyacrylonitrile by potassium hydroxide, Eur. Polym. J. 26 (1990) 9–13. https://doi.org/10.1016/0014-3057(90)90089-M.

[55] M. Jassal, S. Bhowmick, S. Sengupta, P.K. Patra, D.I. Walker, Hydrolyzed Poly(acrylonitrile) Electrospun Ion-Exchange Fibers, Environ. Eng. Sci. 31 (2014) 288–299. https://doi.org/10.1089/ees.2013.0436.

[56] V. Kandjou, A.M. Perez-mas, B. Acevedo, M. Hernaez, A.G. Mayes, S. Melendi-espina, Enhanced covalent p-phenylenediamine crosslinked graphene oxide membranes : Towards superior contaminant removal from wastewaters and improved membrane reusability, J. Hazard. Mater. 380 (2019) 120840. https://doi.org/10.1016/j.jhazmat.2019.120840.

[57] V. Kandjou, M. Hernaez, B. Acevedo, S. Melendi-espina, Interfacial crosslinked controlled thickness graphene oxide thin- fi lms through dip-assisted layer-by-layer assembly means, Prog. Org. Coatings. 137 (2019). https://doi.org/10.1016/j.porgcoat.2019.105345.

[58] V. Kandjou, Z. Gonzalez, B. Acevedo, J.M. Munuera, J.I. Paredes, S. Melendi-espina, Influence of graphene oxide's characteristics on the fabrication and performance of crosslinked nanofiltration membranes, J. Taiwan Inst. Chem. Eng. 000 (2021) 1–8. https://doi.org/10.1016/j.jtice.2021.01.023.

[59] V. Kandjou, M. Hernaez, M.D. Casal, S. Melendi-Espina, Crosslinked graphene oxide membranes: Enhancing membrane material conservation and optimisation, J. Taiwan Inst. Chem. Eng. 136 (2022) 104434. https://doi.org/10.1016/j.jtice.2022.104434.

[60] Z. Jia, Y. Wang, Covalently crosslinked graphene oxide membranes by esterification reactions for ions separation, J. Mater. Chem. A. 3 (2015) 4405–4412. https://doi.org/10.1039/c4ta06193d.

[61] M. Aleksandrzak, P. Adamski, W. Kukulka, B. Zielinska, E. Mijowska, Effect of graphene thickness on photocatalytic activity of TiO2 - graphene nanocomposites, Appl. Surf. Sci. 331 (2015) 193–199. https://doi.org/10.1016/j.apsusc.2015.01.070.

[62] G. Wang, B. Wang, J. Park, J. Yang, X. Shen, J. Yao, Synthesis of enhanced hydrophilic and hydrophobic graphene oxide nanosheets by a solvothermal method, Carbon N. Y. 7 (2008) 6–10. https://doi.org/10.1016/j.carbon.2008.09.002.

[63] C. Hontoria-Lucas, A.. Lopez-Peinado, de D. Lopez-Gonzalez, M.. Cervantes-Rojas, R.. Martin-Aranda, Study of oxygen containing groups in a series of graphite oxides: Physical and Chemical

Characterization, Carbon N. Y. 95 (1995). https://doi.org/10.1016/0008-6223(95)00120-3.

[64] D.C. Marcano, D. V Kosynkin, J.M. Berlin, A. Sinitskii, Z. Sun, A. Slesarev, L.B. Alemany, W. Lu, J.M. Tour, Improved Synthesis of Graphene Oxide, ACS Nano. 4 (2010). https://doi.org/10.1021/nn1006368.

[65] J.I. Paredes, S. Villar-Rodil, A. Martyinez-Alonso, J.M.D. Tascon, Graphene Oxide Dispersions in Organic Solvents, Langmuir. (2008) 10560–10564. https://doi.org/10.1021/la801744a.

[66] X. Liu, N. Wen, X. Wang, Y. Zheng, Layer-by-Layer Self-Assembled Graphene Multilayer Films via Covalent Bonds for Supercapacitor Electrodes, Nanomater. Nanotechnol. 5 (2015) 14. https://doi.org/10.5772/60596.

[67] X. Li, M. Huang, Y. Yang, Synthesis and Characterization of Poly(aniline-co-xylidine)s, Polym. J. 42 (2001). https://doi.org/10.1295/polymj.32.348.

[68] R.H. Sestrem, D.C. Ferreira, R. Landers, M.L.A. Temperini, M. Gustavo, Structure of chemically prepared poly- (para -phenylenediamine) investigated by spectroscopic techniques, Polymer (Guildf). 50 (2009) 6043–6048. https://doi.org/10.1016/j.polymer.2009.10.028.

[69] N.P.G. Roeges, Guide to the complete interpretation of infrared spectra of organic structures, John Wiley and Sons Ltd. Baffins Lane, Chichester, West Sussex, 1994.

[70] N.E. Mircescu, M. Oltean, V. Chis, N. Leopold, FTIR, FT-Raman, SERS and DFT study on melamine, Vib. Spectrosc. 62 (2012) 165–171. https://doi.org/10.1016/j.vibspec.2012.04.008.

[71] R.A. Heacock, L. Marion, The infrared spectra of secondary amines and their salts, Can. J. Chem. 34 (2011) 1782–1795. https://doi.org/10.1139/v56-231.

[72] A.P. Cleaves, E.K. Plyler, The Infra-Red Absorption Spectrum of Methylamine Vapor, J. Chem. Phys. 7 (1939) 563–569. https://doi.org/10.1063/1.1750491.

[73] S. Jawaid, F.N. Talpur, H.I. Afridi, S.M. Nizamani, A.A. Khaskheli, S. Naz, Quick determination of melamine in infant powder and liquid milk by Fourier transform infrared spectroscopy, Anal. Methods. (2014). https://doi.org/10.1039/C4AY00558A.

[74] H. Charville, D.A. Jackson, G. Hodges, A. Whiting, M.R. Wilson, The uncatalyzed direct amide formation reaction - Mechanism studies and the key role of carboxylic acid h-bonding, European J. Org. Chem. (2011) 5981–5990. https://doi.org/10.1002/ejoc.201100714.

[75] R.M. De Figueiredo, J.S. Suppo, J.M. Campagne, Nonclassical Routes for Amide Bond

Formation, Chem. Rev. 116 (2016) 12029–12122. https://doi.org/10.1021/acs.chemrev.6b00237.

[76] N. Azizi, M.R. Saidi, Highly chemoselective addition of amines to epoxides in water, Org. Lett. 7 (2005) 3649–3651. https://doi.org/10.1021/ol051220q.

[77] C. Mateo, V. Grazu, J.M. Palomo, F. Lopez-Gallego, R. Fernandez-Lafuente, J.M. Guisan, Immobilization of enzymes on heterofunctional epoxy supports, Nat. Protoc. 2 (2007) 1022–1033. https://doi.org/10.1038/nprot.2007.133.

[78] W. Gao, Graphene Oxide: Reduction Recipes, Spectroscopy, and Applications, Springer, Cham, 2015. https://doi.org/10.1007/978-3-319-15500-5.

[79] H.L. Ma, H. Bin Zhang, Q.H. Hu, W.J. Li, Z.G. Jiang, Z.Z. Yu, A. Dasari, Functionalization and reduction of graphene oxide with p-phenylene diamine for electrically conductive and thermally stable polystyrene composites, ACS Appl. Mater. Interfaces. 4 (2012) 1948–1953. https://doi.org/10.1021/am201654b.

[80] J. Xia, Y. Zhu, Z. He, F. Wang, H. Wu, Superstrong Noncovalent Interface between Melamine and Graphene Oxide, ACS Appl. Mater. Interfaces. 11 (2019) 17068–17078. https://doi.org/10.1021/acsami.9b02971.

[81] S. Dai, Z. Xu, M. Zhu, Y. Qian, C. Wang, Detection of p-phenylenediamine based on a glassy carbon electrode modified with nitrogen doped graphene, Int. J. Electrochem. Sci. 10 (2015) 7063–7072. https://doi.org/10(9):7063-7072.

[82] P. Monji, R. Jahanmardi, M. Mehranpour, Preparation of melamine-grafted graphene oxide and evaluation of its efficacy as a flame retardant additive for polypropylene, Carbon Lett. 27 (2018) 81–89. https://doi.org/10.5714/CL.2018.27.081.

[83] B. Yuan, H. Sheng, X. Mu, L. Song, Q. Tai, Y. Shi, K.M. Liew, Y. Hu, Enhanced flame retardancy of polypropylene by melamine-modified graphene oxide, J. Mater. Sci. 50 (2015) 5389–5401. https://doi.org/10.1007/s10853-015-9083-0.

[84] V. Georgakilas, J.N. Tiwari, K.C. Kemp, A.B. Perman, Jason A. Bourlinos, K.S. Kim, R. Zboril, Noncovalent Functionalization of Graphene and Graphene Oxide for Energy Materials, Biosensing, Catalytic, and Biomedical Applications, Chem. Rev. 116 (2016) 5464–5519. https://doi.org/10.1021/acs.chemrev.5b00620.

[85] Y. Wei, Y. Zhang, X. Gao, Z. Ma, X. Wang, C. Gao, Multilayered graphene oxide membranes for water treatment: A review, Carbon N. Y. 139 (2018) 964–982.

https://doi.org/10.1016/j.carbon.2018.07.040.

[86] Z. Jia, Y. Wang, W. Shi, J. Wang, Diamines cross-linked graphene oxide free-standing membranes for ion dialysis separation, J. Memb. Sci. 520 (2016) 139–144. https://doi.org/10.1016/j.memsci.2016.07.042.

[87] R.K. Bharadwaj, Modeling the barrier properties of polymer-layered silicate nanocomposites, Macromolecules. 34 (2001) 9189–9192. https://doi.org/10.1021/ma010780b.

[88] J.Y. Chong, B. Wang, C. Mattevi, K. Li, Dynamic microstructure of graphene oxide membranes and the permeation flux, J. Memb. Sci. 549 (2018) 385–392. https://doi.org/10.1016/j.memsci.2017.12.018.

[89] D.A. Aba Nor Farah, J.Y. Chong, B. Wang, C. Mattevi, K. Li, Graphene Oxide Membranes on ceramic hollow fibers - Microstructural stability and nanofiltration performance, J. Memb. Sci. 484 (2015) 87–94. https://doi.org/10.1016/j.memsci.2015.03.001.

[90] W.P. Lee, A.F. Routh, Why Do Drying Films Crack?, Langmuir. 20 (2004) 9885–9888. https://doi.org/10.1021/la049020v.

HIGHLIGHTS

- Crosslinked graphene oxide nanofiltration membranes were successfully fabricated.
- The significance of crosslinking in membrane nanofiltration performance was evident
- Successful indication of enhanced membrane intactness with crosslinking
- Graphene Oxide Membrane stability improvement with crosslinking is evident also.

Declaration of interests

☒ The authors declare that they have no known competing financial interests or personal relationships that could have appeared to influence the work reported in this paper.

☐The authors declare the following financial interests/personal relationships which may be considered as potential competing interests: